Penerbit Akademia Baru

Journal of Advanced Research in Fluid Mechanics and Thermal Sciences

Journal homepage: www.akademiabaru.com/arfmts.html
ISSN: 2289-7879

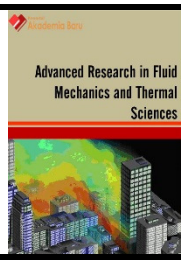

A comparison of cylindrical and row trenched film-cooling holes on a combustor endwall surface at high blowing ratio

Open Access

Ehsan Kianpour[1,*] , Nor Azwadi Che Sidik[2,3]

[1] Department of Mechanical Engineering, Najafabad Branch, Islamic Azad University, Najafabad, Iran
[2] Malaysia-Japan International Institute of Technology (MJIIT), Universiti Teknologi Malaysia Kuala Lumpur, Malaysia
[3] Faculty of Mechanical Engineering, Universiti Teknologi Malaysia, 81310 UTM Skudai, Johor, Malaysia

ARTICLE INFO

Article history:
Received 27 February 2017
Received in revised form 26 March 2017
Accepted 27 March 2017
Available online 28 March 2017

Keywords:
Gas turbine engine, film-cooling, cylindrical hole, trench hole, dilution hole

ABSTRACT

This study was done to study the effects of cylindrical and row trenched cooling holes with alignment angle of ±60 degrees at blowing ratio of BR=3.18 on the film cooling effectiveness near the combustor end wall surface. In this study, a three-dimensional representation of a Pratt and Whitney gas turbine engine was simulated and analysed with a commercial finite volume package FLUENT 6.2.26. The analysis has been carried out with Reynolds-averaged Navier–Stokes turbulence model (RANS) on internal cooling passages. This combustor simulator was combined with the interaction of two rows of dilution jets, which were staggered in the streamwise direction and aligned in the spanwise direction. In comparison with the baseline case of cooling holes, the application of row trenched hole near the endwall surface doubled the performance of film-cooling effectiveness.

1. Introduction

Advanced gas turbine industries are striving for higher engine efficiencies, and Brayton cycle is a key to achieve this purpose. According to this cycle (Figure 1), the turbine inlet temperature should increase to obtain more efficiency. However, the turbine inlet temperature increment formed an extremely harsh environment for critical downstream components such as combustor end wall surface and turbine vanes. Therefore, it is necessary to design a cooling technique in this area. Film cooling is the usual way used. In this system, a thin thermal boundary layer is formed by cooling holes and attached on the protected surface. Cylindrical and trenched cooling holes are two arrangements of the holes. However, to obtain a better film-cooling effectiveness, it is needed to increase blowing ratio because the blowing ratio has a significant effect on the heat transfer, especially in the hole region.

*Corresponding author.
E-mail address: ekianpour@pmc.iaun.ac.ir (Ehsan Kianpour)

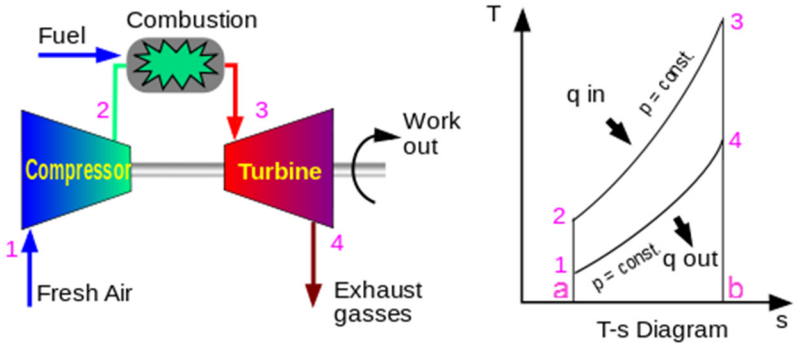

Fig. 1. V-velocity profile along vertical centerline by SIMPLE algorithm at *Re* = 100

Due to the importance of this research, a broad literature survey was conducted to collect the related information. By using large scale, low speed experiments, Rowbury *et al*. [1, 2] detected the effects of flow interaction under the use of annular cascade. They studied the effects of hole geometry, pressure ratio across the hole, and Reynolds number and Mach number on discharge coefficient of coolant. The findings declared that adjacent the end of an injection hole with external cross flow, the static pressure loss relative to the assumed value led to the discharge coefficient enhancement. Vakil and Thole [3] and Barringer *et al*. [4] presented the experimental results of the combustor simulator. They applied a real scale combustor, and the coolant flow and high momentum of dilution jets were injected into the main flow. They found that a high temperature gradient was developed upstream of the dilution holes. Furthermore, the results indicated that the dilution jets reduced the total pressure and velocity fields, and the turbulence level at the end of the combustor reached to 24%. This quantity is a little bit lower compared to the findings of Colban *et al*. [5], which predicted the turbulence level between 25 and 30%. Kianpour *et al*. [6-8] simulated the same model using k-ε and RNG *k-ε* turbulent models to solve the 3-D Navier-Stokes equation. They claimed that the RNG *k-ε* turbulent model was a good choice to detect the variation of temperature in the combustor simulator. This finding was later confirmed by Colban *et al*. [9], Patil *et al*. [10], and Scheepers and Morris [11]. They demonstrated the consistency of the results between experimental and numerical approaches by using the RNG *k-ε* turbulent model.

In another study, Sundaram and Thole [12] and Baheri *et al*. [13] investigated the effects of modified trench depth in order to increase the film cooling effectiveness. The study was conducted with various individual and row trench depths. They reported that maximum cooling effectiveness can be obtained when the trench depth was d= 0.8D (d is the trench depth and D is the diameter of the cooling hole). However, Lawson and Thole [14] found different results, suggesting that this trench depth gives negative effect on the cooling performance downstream the cooling hole. Later, Lu *et al*. [15] and Maikell *et al*. [16] found that the trench depth of d=0.75D gave the optimum efficiency and it was validated by CFD studies. In another study, Barigozzi *et al*. [17] suggested that high efficiency can be obtained when d/D=1.0 but it is restricted to low blowing ratio condition. The effect of blowing ratio on the film cooling efficiency has also attracted few studies.

Somawardhana and Bogard [18] investigated the effects of shallow trenched holes on the turbine vane cascade in the presence of obstructions. The adiabatic effectiveness was calculated for blowing ratios from 0.4 to 1.6. The results indicated that while upstream obstructions reduced the effectiveness by 50%, the downstream obstructions increased the performance of film cooling for all blowing ratios. Furthermore, a combination of both obstructions slightly affected the performance of film cooling and the results were close to the case of upstream obstructions. They also concluded

that the adiabatic effectiveness with the narrow trench was relatively constant across this range of blowing ratios. However, these results were inconsistent with Harrison *et al*. [19], Shuping [20], Baheri Islami and Jurban [21], and Lu and Ekkad [22], which stated that when the blowing ratio increased from 0.6 to 1.4, the performance of the trench was three times greater than that for baseline cylindrical holes. Recently, Ai *et al*. [23] proved that trenching reduced the coolant momentum ratio and impaired the effectiveness while traditional cooling holes performance was better at low blowing ratios.

It appears from the aforementioned investigations that numerous investigations have been conducted on the effects of internal cooling holes. However, no attempt was made to investigate the effects of trenching the cooling holes near the combustor end wall surface on the film cooling effectiveness. The primary zone which senses this high temperature gas is the combustor end wall surface. Developing more effective cooling that covers the area adjacent to the wall is important because without this layer, the outlet combustion temperature increment is not reasonable. It threatens the life of the end wall surface of the combustor and imposes high costing services to the customers. Furthermore, the improvement of film cooling layer adjacent to the combustor end wall surface assists the designers to make better operable condition for the engine, as well as increasing the efficiency. Therefore, the objective of the present study was to investigate the changes of film cooling effectiveness with different arrangements of cooling holes as the baseline case and trenched holes. Also, in order to determine the validity of the results, a comparison between the data gained from this investigation and Vakil and Thole [3] and Stitzel and Thole [24] was made.

2. Research Methodology

In the current research, a 3D representation of a true Pratt and Whitney gas turbine engine was simulated and analysed to obtain fundamental data. Within an actual combustor, the purpose of the film-cooling jets is to provide a cool layer of air that protects the material of the combustor's inner and outer casing. Without this film cooling, the material would surely begin to melt, eventually leading to catastrophic failure. Figure 2 shows the schematic view of the combustor.

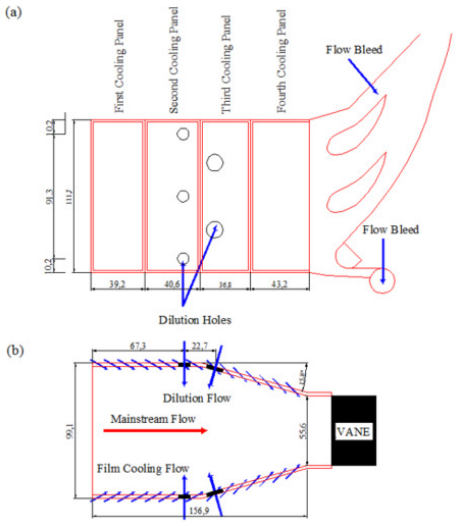

Fig. 2. Schematics of the combustor simulator: (a) top view and (b) side view

The combustor simulator length, width, and inlet height was 156.9 cm, 111.8 cm, and 99.1 cm, respectively. The contraction angle was 15.8 degrees and it began at x = 79.8 cm. While, the inlet

cross-sectional area was 1.11m2, the exit cross-sectional area was 0.62m2. The combustor contained four streamwise film-cooling panels. The combustor simulator consisted of a streamwise series of four film-cooled panels, which were symmetric on the top and bottom of the combustor simulator. These panels began approximately 1.57 m upstream of the turbine test section. The first two panels were flat. They were 39 and 41 cm in length. While the third and fourth panels were 37 cm and 43 cm. The panels were 1.27 cm in thickness. Theses panels were made from low thermal conductivity (k=0.037 W/mk) of combustor panels allowed for adiabatic surface temperature measurements. The second and third cooling panels contained two different rows of dilution holes. These dilution rows were located at 0.67m and 0.90m downstream of the beginning of the combustor liner panels. The first and second row of dilution holes diameter was 8.5 cm and 11.9 cm, respectively. The centerline of the second row was staggered with respect to those of the first row. In the present research, the combustor simulator included three configurations of cooling holes. For the verification of findings, the first arrangement (baseline or case 1) was planned similar to the Vakil and Thole [3] combustor simulator. For all cases, the cooling holes were located in equilateral triangles. The diameter of the cooling holes was 0.76 cm and drilled at an angle of 30 degrees from the horizontal surface. The length of each cooling holes in the baseline case was 2.5 cm. For the second and third cases shown in Figure 3, the cooling holes were placed within a row trench with alignment angle of +60 degrees (case 2) and -60 degrees (case 3).

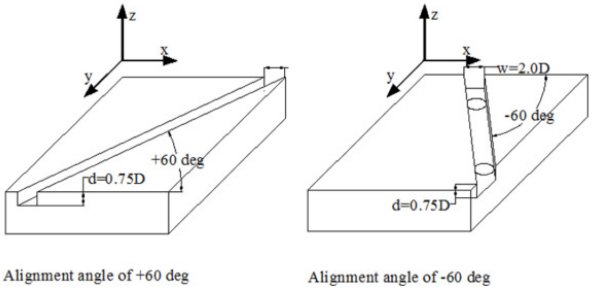

Fig. 3. Arrangements of trenched cooling holes with different alignment angles

According to the Yiping *et al*. [25], Lawson and Thole [14], and Sundaram and Thole [12] findings, the trench depth and width was considered equal to 0.75D and 1.0 D, respectively. These researchers showed that the optimum film-cooling effectiveness for the trenched cases was obtained among the narrower trench and the depth of d=0.75D. Furthermore, a coolant blowing ratios of BR=3.18 was considered. A global coordinate system (x, y, and z) was also selected. In comparing the results, a number of non-dimensional parameters were needed to be made. The dimensionless variables were defined for both the coolant and the dilution flow. Table 1 gives a complete description of the operating conditions for the main flow and table 2 shows non-dimensional parameters of the dilution jets and coolant, respectively. In addition, the coolant and dilution jets temperature was considered equal to 295.5 K. The distribution of film-cooling effectiveness inside the combustor simulator was measured along the specific observation planes.

The observation planes are shown in Figures 4(a) (baseline), 4(b) (case 2), and 4(c) (case 3). The flow field observation planes of 0p, 1p, 2p, and 3p were located in pitchwise direction and the observation plane of 0s was placed in the streamwise direction. Plane 0p was placed exactly downstream of the first panel of cooling holes and at x=35.1 cm. The momentum distribution of film cooling was determined along this panel. This observation plane covered half of the combustor simulator in the spanwise direction. The height of the observation plane covered 0 cm<z<10 cm.

Plane 1p was placed downstream of the first row of dilution jet at x=74.85 cm. This plane was expanded from z=0 cm to z=10 cm and covered the half width of the combustor simulator. This plane was used to detect the effects of film cooling on the dilution flow. This plane was also used to determine the effects of horseshoe, half-wake, and counter rotating vortexes. Plane 2p was located downstream of the trailing edge of the second row of dilution holes. This plane was embedded at x=1.1 cm and was expanded along the vertical axis from z=0.09 cm to 0.22 cm. The effects of the cooling holes located in this section on the thermal behaviour were identified by this plane using. Plane 3p was set at the end of combustor simulator. The usage of this plane enabled the researcher to detect the exit flow behaviour and the varying temperature of the combustor. Plane 0s was located directly at the central point of the first row of dilution jet at y=9.3 cm and covered from x=39.2 cm to x=78.45 cm. This plane was used to analyse the interaction of flow along the first row of dilution jets.

Table 1
Typical operating condition for main flow

Parameter	Quantity
Main Flow Pressure (Kilo Pascal)	98.82
Main Flow Temperature (K)	332
Main Flow Velocity (m/s)	1.62
Main Flow Density (kg/m^3)	1.0

Table 2
Dimensional flow parameters for coolant and dilution jets

Parameter	Location	Combustor simulator
Density (kg/m^3)	Main Flow	1
	Dilution row 1	1.12
	Dilution row 2	1.12
	Cooling panels	1.12
Velocity (m/s)	Main Flow	1.62
	Dilution row 1	17.36
	Dilution row 2	8.68
	Cooling panels	4.6
Temperature (K)	Main Flow	332
	Dilution row 1	295.5
	Dilution row 2	295.5
	Cooling panels	295.5
Pressure (kPa)	Main Flow	98.82

About 8×10^6 tetrahedral meshes were needed to solve the combustor simulator problem and to get more accurate data in inappropriate time. The usage of this number of meshes allowed adequate convergence for refined meshing. The precision of the number of meshes used in this research was in agreement with a study by Stitzel and Thole [24]. The meshes were denser around the cooling and dilution holes as well as wall surfaces (Figure 5).

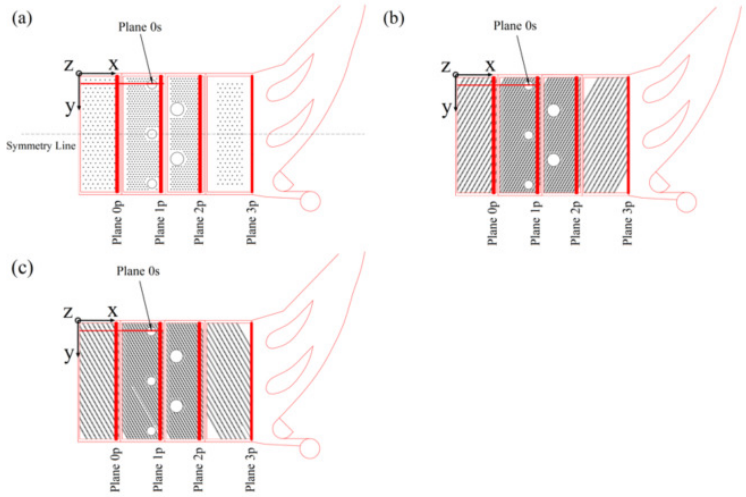

Fig. 4. Location of the observation planes: (a) baseline, (b) case 2, and (c) case 3

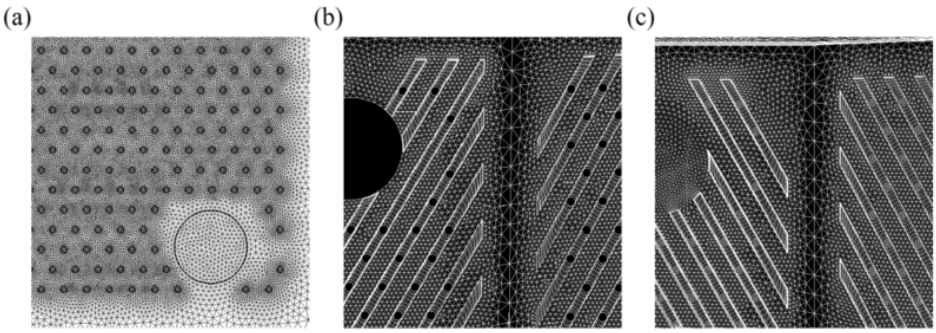

Fig. 5. 3D meshes of combustor simulator (a) baseline case (b) Case 2 (c) case

According to the specific blowing ratio at the inlet of volume control, inlet mass flow boundary condition was considered at the inlet. Wall boundary condition and slip-less boundary condition were used to limit the interaction zone between fluid and solid layer. In addition, to compare the outcomes of the present research with the previous findings as reported [3,24,26], the inlet flow boundary was set as uniform flow and pressure outlet at the exit. Totally, according to the symmetries of the Pratt and Whitney gas turbine engine combustor, symmetry boundary condition was used. By using the Gambit software, the combustor simulator was meshed and data were simulated and analysed by using Fluent 6.2.26 software. The results were gathered in the form of charts and different contours. The results were cross-checked with the findings obtained by Vakil and Thole [3] and Stitzel and Thole [24] researches to calculate the validity of the findings.

The numerical method considered a transient, incompressible turbulent flow by means of the *k*–*ε* turbulent model of the Navier–Stokes equations expressed as follows:

Continuity equation

$$\frac{\partial}{\partial t}(\rho u_i) + \frac{\partial}{\partial x_j} = (\rho u_i u_j) = -\frac{\partial P}{\partial x_i} + \frac{\partial \tau_{ij}}{\partial x_i} + \rho g_i + \overrightarrow{F_i} \quad (1)$$

Momentum equation

$$\frac{\partial \rho}{\partial t} + \frac{\partial}{\partial x}\frac{dx}{dt} + \frac{\partial \rho}{\partial y}\frac{dy}{dt} + \frac{\partial \rho}{\partial z}\frac{dz}{dt} = -\rho(\nabla . V) \quad (2)$$

Energy equation

$$\frac{\partial}{\partial t}(\rho E)+\frac{\partial}{\partial x_i}\left(u_i(\rho E+P)\right)=\frac{\partial}{\partial x_i}\left(K_{eff}\frac{\partial T}{\partial x_i}-\sum_j h_j J_j+u_j(\tau_{ij})_{erf}\right)+S_h \quad (3)$$

and k–ε equation

$$\frac{\partial}{\partial t}(\rho k)+\frac{\partial}{\partial x_i}(\rho k u_i)=\frac{\partial}{\partial x_j}\left[\left(\mu+\frac{\mu_t}{\sigma_k}\right)\frac{\partial k}{\partial x_j}\right]+P_k-\rho\varepsilon \quad (4)$$

$$\frac{\partial}{\partial t}(\rho \varepsilon)+\frac{\partial}{\partial x_i}(\rho \varepsilon u_i)=\frac{\partial}{\partial x_j}\left[\left(\mu+\frac{\mu_t}{\sigma_\varepsilon}\right)\frac{\partial \varepsilon}{\partial x_j}\right]+C_{1\varepsilon}\frac{\varepsilon}{k}P_k-C_{2\varepsilon}^{*}\rho\frac{\varepsilon^2}{k} \quad (5)$$

The first-order upwind and central differencing scheme were used to approximate the convective and diffusion terms in the differential equation, respectively. To check the convergence, the mass residue of each control volume has been calculated and the maximum value has been used to check for the convergence. The convergence criterion has been set to 10^{-4}. Film-cooling effectiveness is defined as below:

$$\eta=\frac{T-T_\infty}{T_C-T_\infty} \quad (6)$$

In the above equation, T is the local temperature, T_∞ is main stream temperature, and T_C is the temperature of coolant.

3. Results and discussion

The comparison was done between the current study results and the experimental results collected by Vakil and Thole [3] and numerical findings gathered by Stitzel and Thole [24]. Figure 6 shows the comparison of film-cooling effectiveness for plane 1p and 2p at y/W=0.4. Deviations between the current computation and benchmarks were calculated as follows:

$$\%\text{Diff}=\frac{\sum_{i=1}^{n}\frac{x_i-x_{i,benchmark}}{x_{i,benchmark}}}{n}\times 100 \quad (7)$$

According to this equation, the deviation estimation was 9.76% and 8.34% compared to Ref [3] and Ref [24] for plane 1p and equal to 13.36% and 11.96% in comparison with Ref [3] and Ref [24] for plane 2p.

Figure 7 shows the findings of the film cooling effectiveness made for plane 0p. The observation plane was located at x/L=0.24, which was two film-cooling hole diameters (2d) downstream of the trailing edge of the last row of the cooling holes in panel one. A major difference between these figures is the film-cooling layer thickness. While, for the trenched cooling holes with alignment angle of +60 degrees, the thickness of this layer reached to z=50mm, for the baseline and trenched holes with alignment angle of -60 degrees, it reached to z=10 mm and z=4mm respectively. However, for this measurement plane, the thicker film-cooling layer for the trenched hole does not automatically suggested that it is desirable. As seen in the figure, by increasing the blowing ratio led to a better protection over the end wall surface. Of course, for the trenched case with alignment angle of +60 degrees and at a position of 28cm<y<42cm, the temperature level was higher (0.2<η<0.25) near the end wall surface.

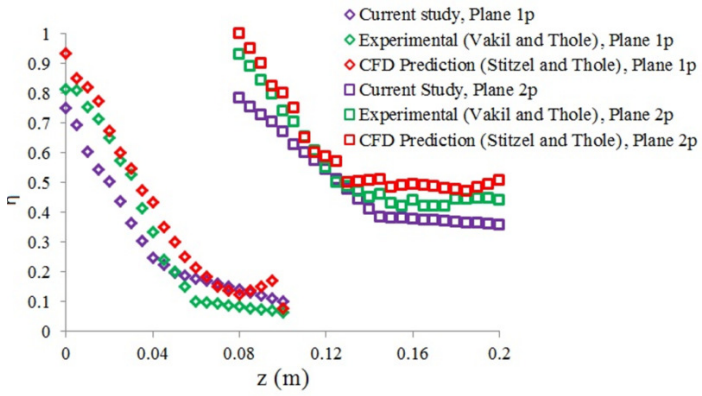

Fig. 6. The film cooling effectiveness comparison of planes 1p and 2p along y/W=0.4

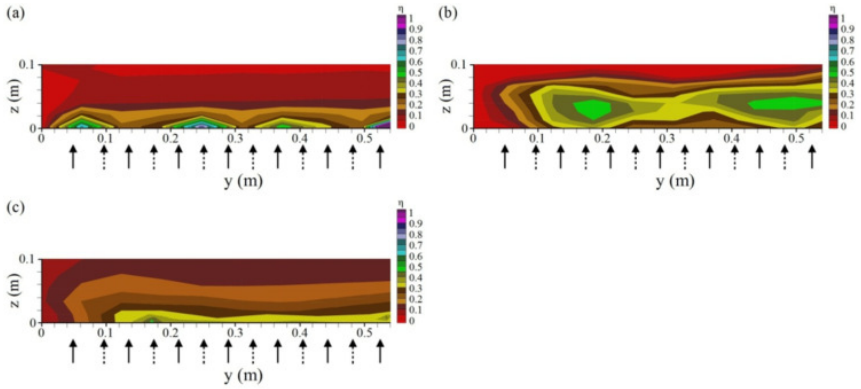

Fig. 7. Film-cooling effectiveness of plane 0p (a) baseline (b) case 2 (c) case 3

The distribution of film-cooling effectiveness for plane 1p is shown in Figure 8. Plane 1p was taken directly downstream of the first row of the dilution jets. This particular hole is centrally located right at the mid pitch within the combustor simulator. Note that, the film-cooling effectiveness was significantly increased for the trench cases, especially for the trenched holes with alignment angle of +60 degrees. On the right side (50 cm<y<54 cm) of thermal field contours and for the trenched cases, film cooling was being entrained by the upward motion of dilution jet. Furthermore, at the positions of 18cm<y<40cm and 8cm<z<10cm were slightly hotter (0<η<0.05) for the case 2 as well as 44cm<y<49cm and 8cm<z<10cm for the baseline case.

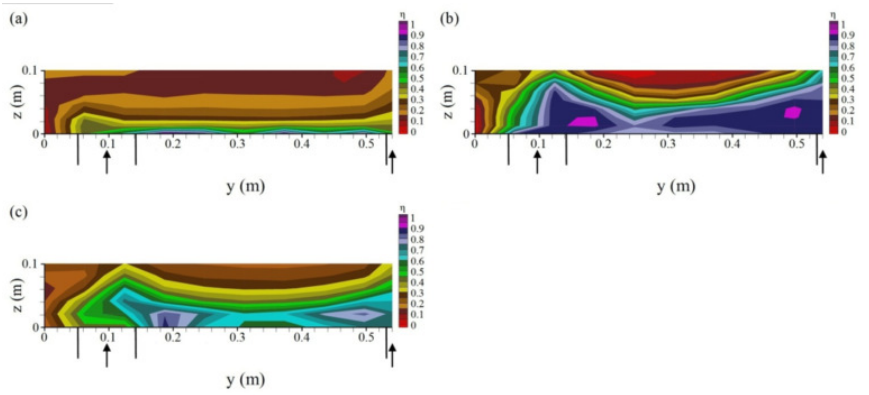

Fig. 8. Film-cooling effectiveness of plane 0p (a) baseline (b) case 2 (c) case 3

Figure 9 shows the film-cooling effectiveness distribution for plane 2p for three different configurations of baseline case and row trenched cooling holes with alignment angles of ±60 degrees. It is declared from the analysis of contours that the rotating flow is seen on the left side of the figure. It is entrained along the spanwise direction. However, with trenching cooling holes, this rotating flow is growing; especially in the trenched case with alignment an angle of +60 degrees. Overwhelmingly apparent, however, is the lack of uniformity within the combustor exiting profile at this point. At the right side of Figure 9(a), the hot gases also covered more extended area in comparison with trenched cases as well as at the right side of the temperature distribution contour of trenched holes with an alignment angle of +60 degrees. Lastly, these figures showed the v and w velocity vectors superimposed on the thermal field contours of this measurement plane. The sweeping of the coolant toward the second row of dilution jet is visible in all cases.

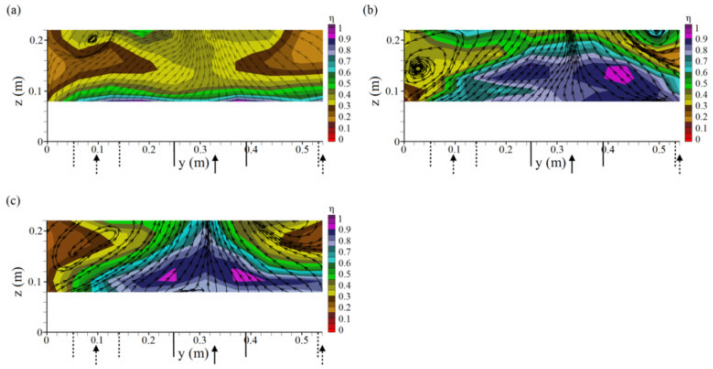

Fig. 9. Film-cooling effectiveness in plane 2p (a) baseline (b) case 2 (c) case 3

Figure 10 indicates the film-cooling effectiveness distribution of plane 3p. The results showed that with trenching the cooling holes, the baseline case showed a better performance and film-cooling effectiveness is higher ($0.6<\eta<0.75$) than others.

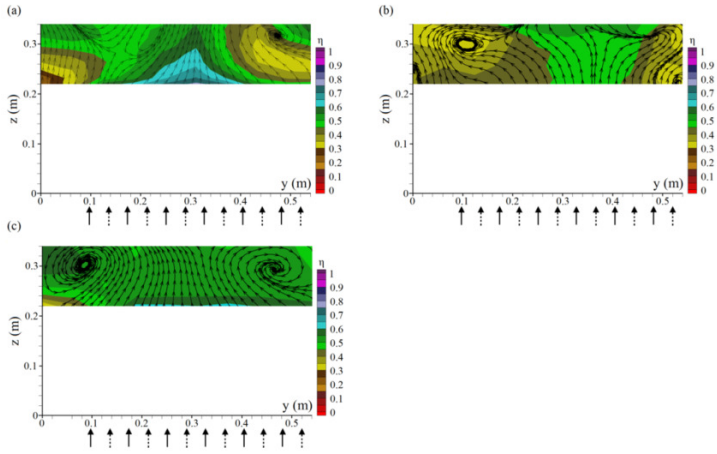

Fig. 10. Film-cooling effectiveness in plane 2p (a) baseline (b) case 2 (c) case 3

Furthermore, for the row trenched hole with alignment angle of +60 degrees, the hot gases were spread from the corners of contours to the central part and affect the cooling. This figure also shows case 3 (trench holes with alignment angle of -60 degrees) has better effect on the film cooling

effectiveness than case 2 and also the temperature variation of flow is more uniform in this case. The velocity vectors of v and w overlying on the thermal field contours in plane 3p. A dominant vortex, rotating in the counter-clockwise direction at 48<y<54 cm was clearly illustrated within this figure. The clockwise rotating vortex is only found at 7 cm<y<20 cm in all cases. Of course, the rotating of the vortex is more turbulent for the trenched cases because the coolant was injected further and the interaction of the film-coolant flow was entrained by the shear forces created by the main flow.

4. Conclusion

The purpose of this research was to analyse the effects of different holes arrangements as baseline and row trench cases with alignment angles of ±60 degrees on the film-cooling effectiveness at the end of combustor simulator and near the end wall surface. In the present study, a three-dimensional representation of a true Pratt and Whitney gas turbine engine was analysed with a commercial finite volume package Fluent 6.2.26. As a summary for all schemes, the film-cooling layer is growing at elevated blowing ratio; it was thinned by using the cylindrical holes for plane 2p. In addition, the central section of the plane 2p declared severe penetration of the cooling jets and a thick film-cooling layer creation for the trenched layouts, especially for the trenched hole with alignment angle of +60 degrees. On the other hand, blowing ratio increase led to a cooler region near the wall and between the jets. The thermal field outcomes indicated a recirculation area extended at exactly downstream of the jet where the entrainment of film cooling was occurred by the dilution jet. The streamwise thermal field contours indicated a strong effect of trenched cooling holes and dilution injection downstream the dilution jet, especially for the trenched holes. For the measurement plane of 0p, 1p and 2p, the film-cooling effectiveness enhancement happened with using row trench cooling holes. While, for the plane 3p, the film-cooling performance decreased for the trench cases. Based on the results and conclusions of the study, there are several recommendations to notice. In later researches within this field of study, it is strongly recommended to use the trenched holes for the second and third cooling panels because trenching cooling holes have a better effect on film-cooling performance at higher blowing ratios.

References

[1] Rowbury, D. A., M. L. G. Oldfield, and G. D. Lock. "Large-scale testing to validate the influence of external crossflow on the discharge coefficients of film cooling holes." In ASME Turbo Expo 2000: Power for Land, Sea, and Air, pp. V003T01A094-V003T01A094. American Society of Mechanical Engineers, 2000.

[2] Rowbury, D. A., M. L. G. Oldfield, and G. D. Lock. "A method for correlating the influence of external crossflow on the discharge coefficients of film cooling holes." In ASME Turbo Expo 2000: Power for Land, Sea, and Air, pp. V003T01A095-V003T01A095. American Society of Mechanical Engineers, 2000.

[3] Vakil, Sachin Suresh, and K. A. Thole. "Flow and Thermal Field Measurements in a Combustor Simulator Relevant to a Gas Turbine Aero-Engine." In ASME Turbo Expo 2003, collocated with the 2003 International Joint Power Generation Conference, pp. 215-224. American Society of Mechanical Engineers, 2003.

[4] Barringer, M. D., O. T. Richard, J. P. Walter, S. M. Stitzel, and K. A. Thole. "Flow field simulations of a gas turbine combustor." In ASME Turbo Expo 2001: Power for Land, Sea, and Air, pp. V003T01A048-V003T01A048. American Society of Mechanical Engineers, 2001.

[5] Colban, W. F., A. T. Lethander, K. A. Thole, and G. Zess. "Combustor Turbine Interface Studies: Part 2—Flow and Thermal Field Measurements." In ASME Turbo Expo 2002: Power for Land, Sea, and Air, pp. 1003-1009. American Society of Mechanical Engineers, 2002.

[6] Kianpour, Ehsan, Nor Azwadi Che Sidik, and Iman Golshokouh. "Measurement of Film Effectiveness for Cylindrical and Row Trenched Cooling Holes at Different Blowing Ratios." Numerical Heat Transfer, Part A: Applications 66, no. 10 (2014): 1154-1171.

[7] Azwadi, Nor, and Ehsan Kianpour. "The Effect of Blowing Ratio on Film Cooling Effectiveness Using Cylindrical and Row Trenched Cooling Holes with Alignment Angle of 90 Degrees." Mathematical Problems in Engineering 2014 (2014).

[8] Kianpour, Ehsan, Nor Awadi C. Sidik, and Mazlan Abdul Wahid. "Cylindrical and Row Trenched Cooling Holes with Alignment Angle of 90 Degree at Different Blowing Ratios." CFD Letters 5, no. 4 (2013): 165-173.
[9] Colban, W., A. Gratton, K. A. Thole, and M. Haendler. "Heat transfer and film-cooling measurements on a stator vane with fan-shaped cooling holes." *Journal of Turbomachinery* 128, no. 1 (2006): 53-61.
[10] Patil, Sunil, Santosh Abraham, Danesh Tafti, Srinath Ekkad, Yong Kim, Partha Dutta, Hee-Koo Moon, and Ram Srinivasan. "Experimental and numerical investigation of convective heat transfer in a gas turbine can combustor." *Journal of Turbomachinery* 133, no. 1 (2011): 011028.
[11] Scheepers, Gerard, and R. M. Morris. "Experimental study of heat transfer augmentation near the entrance to a film cooling hole in a turbine blade cooling passage." *Journal of Turbomachinery* 131, no. 4 (2009): 044501.
[12] Sundaram, N., and K. A. Thole. "Bump and trench modifications to film-cooling holes at the vane-endwall junction." *Journal of Turbomachinery* 130, no. 4 (2008): 041013.
[13] Baheri, S., SP Alavi Tabrizi, and B. A. Jubran. "Film cooling effectiveness from trenched shaped and compound holes." *Heat and Mass Transfer* 44, no. 8 (2008): 989-998.
[14] Lawson, Seth A., and Karen A. Thole. "Simulations of Multiphase Particle Deposition on Endwall Film-Cooling Holes in Transverse Trenches." *Journal of Turbomachinery* 134, no. 5 (2012): 051040.
[15] Lu, Yiping, Alok Dhungel, Srinath V. Ekkad, and Ronald S. Bunker. "Effect of trench width and depth on film cooling from cylindrical holes embedded in trenches." *Journal of Turbomachinery* 131, no. 1 (2009): 011003.
[16] Maikell, Jonathan, David Bogard, Justin Piggush, and Atul Kohli. "Experimental simulation of a film cooled turbine blade leading edge including thermal barrier coating effects." *Journal of Turbomachinery* 133, no. 1 (2011): 011014.
[17] Barigozzi, Giovanna, Giuseppe Franchini, Antonio Perdichizzi, and Silvia Ravelli. "Effects of trenched holes on film cooling of a contoured endwall nozzle vane." *Journal of Turbomachinery* 134, no. 4 (2012): 041009.
[18] Somawardhana, Ruwan P., and David G. Bogard. "Effects of obstructions and surface roughness on film cooling effectiveness with and without a transverse trench." *Journal of Turbomachinery* 131, no. 1 (2009): 011010.
[19] Harrison, Katharine L., John R. Dorrington, Jason E. Dees, David G. Bogard, and Ronald S. Bunker. "Turbine airfoil net heat flux reduction with cylindrical holes embedded in a transverse trench." *Journal of Turbomachinery* 131, no. 1 (2009): 011012.
[20] Chen, Shuping. "Film cooling enhancement with surface restructure." PhD diss., University of Pittsburgh, 2009.
[21] Islami, S. Baheri, and B. A. Jubran. "The effect of turbulence intensity on film cooling of gas turbine blade from trenched shaped holes." *Heat and Mass Transfer* 48, no. 5 (2012): 831-840.
[22] Lu, Yiping, and Srinath Ekkad. "Predictions of film cooling from cylindrical holes embedded in trenches." In *9th AIAA/ASME Joint Thermophysics and Heat Transfer Conference*, p. 3401. 2006.
[23] Ai, Weiguo, Robert G. Laycock, Devin S. Rappleye, Thomas H. Fletcher, and Jeffrey P. Bons. "Effect of particle size and trench configuration on deposition from fine coal flyash near film cooling holes." *Energy & Fuels* 25, no. 3 (2011): 1066-1076.
[24] Colban, W., K. A. Thole, and M. Haendler. "A comparison of cylindrical and fan-shaped film-cooling holes on a vane endwall at low and high freestream turbulence levels." *Journal of Turbomachinery* 130, no. 3 (2008): 031007.
[25] Stitzel, Sarah, and Karen A. Thole. "Flow field computations of combustor-turbine interactions relevant to a gas turbine engine." In *ASME Turbo Expo 2003, collocated with the 2003 International Joint Power Generation Conference*, pp. 175-183. American Society of Mechanical Engineers, 2003.
[26] Lu, Yiping, Alok Dhungel, Srinath V. Ekkad, and Ronald S. Bunker. "Effect of trench width and depth on film cooling from cylindrical holes embedded in trenches." *Journal of Turbomachinery* 131, no. 1 (2009): 011003.
[27] Stitzel, Sarah, and Karen A. Thole. "Flow field computations of combustor-turbine interactions relevant to a gas turbine engine." In *ASME Turbo Expo 2003, collocated with the 2003 International Joint Power Generation Conference*, pp. 175-183. American Society of Mechanical Engineers, 2003.